NUMERICAL SIMULATION OF ADVECTIVE LOTKA-VOLTERRA SYSTEMS BY DISCONTINUOUS GALERKIN METHOD

A THESIS SUBMITTED TO
THE GRADUATE SCHOOL OF APPLIED MATHEMATICS
OF
MIDDLE EAST TECHNICAL UNIVERSITY

BY

SENEM AKTAŞ

IN PARTIAL FULFILLMENT OF THE REQUIREMENTS
FOR
THE DEGREE OF MASTER OF SCIENCE
IN
SCIENTIFIC COMPUTING

FEBRUARY 2015

Approval of the thesis:

NUMERICAL SIMULATION OF ADVECTIVE LOTKA-VOLTERRA SYSTEMS BY DISCONTINUOUS GALERKIN METHOD

submitted by **SENEM AKTAŞ** in partial fulfillment of the requirements for the degree of **Master of Science in Department of Scientific Computing, Middle East Technical University** by,

Prof. Dr. Bülent Karasözen
Director, Graduate School of **Applied Mathematics** _____

Prof. Dr. Bülent Karasözen
Head of Department, **Scientific Computing** _____

Prof. Dr. Bülent Karasözen
Supervisor, **Institute of Applied Mathematics, METU** _____

Dr. Murat Uzunca
Co-supervisor, **Mathematics Department, Atılım University** _____

Examining Committee Members:

Prof. Dr. Gerhard Wilhelm Weber
Institute of Applied Mathematics, METU _____

Prof. Dr. Bülent Karasözen
Institute of Applied Mathematics, METU _____

Assoc. Prof. Dr. Ömür Uğur
Institute of Applied Mathematics, METU _____

Assoc. Prof. Dr. Sevtap Selçuk-Kestel
Institute of Applied Mathematics, METU _____

Dr. Murat Uzunca
Mathematics Department, Atılım University _____

Date: _____

I hereby declare that all information in this document has been obtained and presented in accordance with academic rules and ethical conduct. I also declare that, as required by these rules and conduct, I have fully cited and referenced all material and results that are not original to this work.

Name, Last Name: SENEM AKTAŞ

Signature :

ABSTRACT

NUMERICAL SIMULATION OF ADVECTIVE LOTKA-VOLTERRA SYSTEMS BY DISCONTINUOUS GALERKIN METHOD

Aktaş, Senem

M.S., Department of Scientific Computing

Supervisor : Prof. Dr. Bülent Karasözen

Co-Supervisor : Dr. Murat Uzunca

February 2015, 35 pages

In this thesis, we study numerically advection-diffusion-reaction equations arising from Lotka-Volterra models in river ecosystems characterized by unidirectional flow. We consider two and three species models which include competition, coexistence and extinction depending on the parameters. The one dimensional models are discretized by interior penalty discontinuous Galerkin model in space. For time discretization, fully implicit backward Euler method and semi-implicit IMEX-BDF methods are used. Numerical simulations for various set up parameters reveal more insight in the complicated dynamics by advective Lotka-Volterra systems.

Keywords : Convection-diffusion-reaction equation, Lotka-Volterra equations, Discontinuous Galerkin, Implicit Euler, IMEX method

ÖZ

ADVEKSİYONLU LOTKA-VOLTERRA DENKLEMLERİNİN KESİNTİLİ GALERKİN YÖNTEMLEİYLE NÜMERİK SİMÜLASYONU

Aktaş, Senem

Yüksek Lisans, Bilimsel Hesaplama Bölümü

Tez Yöneticisi : Prof. Dr. Bülent Karasözen

Ortak Tez Yöneticisi : Dr. Murat Uzunca

Şubat 2015, 35 sayfa

Bu tezde adveksiyon terimi içeren Lotka-Volterra denklemleri, tek yönlü akış ile nitelendirilmiş nehir ekosistemlerinde ele alınmıştır. Değişkenlere bağlı olarak rekabet, bir arada varolma ve yok olma durumlarını içeren iki ve üç türlü modellerin davranışları sayısal olarak incelenmektedir. Bu denklemler uzayda kesintili Galerkin yöntemi kullanılarak ayrıklaştırılmıştır. Zaman ayrıklaştırılması için kapalı Euler yöntemi ve yarı kapalı IMEX-BDF yöntemi kullanılmıştır. Çeşitli değişkenler ile yapılan nümerik simülasyonlar adveksiyonlu Lotka-Volterra sistemlerinin karmaşık dinamik yapısının daha iyi anlaşılmasını sağlamıştır.

Anahtar Kelimeler: Konveksiyon-difüzyon-reaksion denklemi, Lotka-Volterra denklemleri, Süreksiz Galerkin yöntemi, Kapalı Euler yöntemi, IMEX yöntemi

To My Family

ACKNOWLEDGMENTS

I thank my supervisor Prof. Dr. Bülent Karasözen for giving me the possibility to do the necessary research work and for guiding me through my graduate study in our institute.

Finally, I owe special thanks to my co-supervisor Dr. Murat Uzunca who gave me huge support to complete this thesis.

TABLE OF CONTENTS

LIST OF FIGURES

CHAPTER 1

INTRODUCTION

Advection is a movement mechanism of a substance in an environment like water or air. Diffusion refers to the net movement of a substance from high concentration to low concentration and reaction is the response to an action that results in the interconversion of species. The advection-diffusion-reaction(ADR) model describes the density changes of substances under the effects of these three parameters. ADR equations are used as model in different applications. Examples of ADR equations are the transform of water steam in the Earth's atmosphere [20], the pollution of air and water and the effects of unidirectional flow on the spatial models of community composition [12, 25] and nuclear contamination [11]. Moreover, species replacement in river ecosystems is another area where these equations are applied [15].

ADR equations coupled by Lotka-Volterra(LV) interaction terms are discussed in [15], whereas dynamical behavior of advective Lotka-Volterra equations with three species are analyzed in detail in [30].

In this thesis, we consider the following coupled system of ADR equations [13]:

$$\frac{\partial u_i}{\partial t} + v \cdot \nabla u_i - d_i \Delta u_i + R_i(u_1, \ldots, u_m) = f_i(x,t), \text{ on } \Omega \times J,\ i = 1, 2, \ldots, m, \quad (1.1)$$

where $J = (0, T)$, Ω is a bounded domain in $\mathbb{R}^1$ or $\mathbb{R}^2$ with a smooth or piecewise boundary, v is the velocity vector in $\mathbb{R}^d$ for $d = 1, 2$ and d_i's are diffusion parameters. R_i's and $f_i(x,t)$'s denote the nonlinear reaction terms and the source terms, respectively. The unknowns u_i's denote the concentrations or densities of the corresponding species, ∇ stays for the gradient operator and Δ denotes the Laplace operator. In these equations, advection and diffusion terms which are v and d_i respectively constitute the linear part of our general system. On the other hand, reaction term are the nonlinear part of our general system.

The numerical approximations to the solutions of the ADR models are studied intensively using finite differences, finite volume and finite elements methods. A finite volume algorithm on the sphere was derived by Pudykiewicz [18]. Because the resulting discretized systems are very large, efficient numerical integrator and nonlinear solvers are needed. A pseudo-non-time splitting method was introduced by Sun [26] by proving the convergence, stability of the approximate solutions and giving priori error estimates. Different operator splitting methods and parallelization techniques are applied

to the ADR equations. A summary of applications in environmental engineering are solved by the continuous finite elements, theoretical and numerical convergence rates are presented in [13]. Discontinuous Galerkin(DG) methods have also been used in these equations [5]. Finite difference methods can not be applied easily to complex geometries, finite volume methods do not have higher order accuracies and finite element methods are not locally mass conservative for ADR equations. However, DG provides all of these properties. Moroever, because of its compact formulation, it can be applied near boundaries without any special treatment. Hence, it increases the robustness and accuracy.

An important class of ADR equations are the advective Lotka-Volterra equations. In 1925, Lotka firstly proposed these equations on prey-predator models [14]. Volterra also found the same equations as independent drom Lotka [31]. Uniqueness of a positive solution to LV models was proven by Hrinca [2]. Dynamical properties and condition for the coexistence and extinction of the species of the advective Lokta-Volterra equations in an uni-directional flow was investigated in detail in [15, 30]. In this thesis, we study the numerical approximation of one and two dimensional ADR equations, discretizing them in space by interior penalty Galerkin method [3, 21]. For time discretization we use the implicit backward Euler method and the two-step semi-implicit backward differentiation formula IMEX-BDF [1].

Time discretization methods for ADR equations is another field of study since ADR equations are time dependent problems. Many time splitting methods have been applied to these equations [28, 26]. Backward Euler method is a fully implicit method which has been used for ADR equations [29].

The paper organized as follows. In Chapter 2, we give the advective Lotka-Volterra model as a system of diffusion-convection-reaction equations. In Chapter 3, the interior Galerkin discretizations of the ADR equations for 1 dimensional and 2 dimensinol problems are presented in general form. Time discretization is summarized in Chapter 4. In addition to a fully implicit backward Euler method, a semi-implicit IMEX-BDF(backward differential) method is also given in this chapter. Numerical results for a coupled system of four ADR equations with chemically interacting species, and two and three species advective Lotka-Volterra equations are presented in Chapter 4.

CHAPTER 2

ADVECTIVE LOTKA-VOLTERRA EQUATIONS

Proposed by Lotka and Volterra, the well known Lotka-Volterra models concerning ecological population dynamics have been extensively studied in the literature as a model for oscillating chemical reactions in 1910. In 1920, a plant species and a herbivorous animal species were used to range the model to organic system by Lotka and in 1925, Lotka also used the equations in [14] to analyze predator-prey interactions on biomathematics and the equations took the today's form. As independent from Lotka, Vito Volterra [31] made a statistical analysis of fish catches in the Adriatic, so he also found the equations in 1926.

Since that time, Lotka-Volterra model has been used in many problems such as population biology [27], chemical kinetics, neural networks [17], in epidemiology and it has become a classic model for nonlinear dynamical systems. This model was extended with offering the idea of functional response by C.S.Holling [7, 8]. Analytical methods are usually known for Lotka-Volterra equations. One of these method is Adomian decomposition method [23] which was introduced by Adomian in 1980's. It provides approximate analytical solutions in the form of an infinite series for nonlinear equations by avoiding linerization, discretization and scientifically unrealistic assumptions. Apart from analytic methods, numerical methods are also used in Lotka-Volterra models. In [16], Mickens shows a non-standard finite difference scheme for the Lotka-Volterra system. An asymptotic approach of Taylor truncated series is used by Scarpello and Ritelli in [24].

The uniqueness of a positive solution to a Lotka-Volterra System with diffusion with two species was proved by Hrinca and he also accomplished boundness analysis of the solution [2]. Kishimoto [10] studied examples of the diffusive three species Lotka-Volterra system by using stable spatially nonconstant equilibrium solutions. Two ADR equations coupled by Lotka-Volterra interaction terms are discussed in [15], whereas dynamical behavior of advective Lotka-Volterra equations with three species are analyzed in detail in [30].

2.1 Model: Two Competing Species Advective LV Model

In [15], LV model is developed with the diffusive, advective flow and spatial varying growth rates. Assume that of two competing species at time $t \geq 0$. Two species advective LV equations $U_{1,2}(t,x)$ denote respective densities take the form:

$$\begin{aligned} \frac{\partial U_1}{\partial t} &= D_1 \frac{\partial^2 U_1}{\partial x^2} - V_1 \frac{\partial U_1}{\partial x} + U_1(R_1(x) - A_{11}U_1 - A_{12}U_2), \\ \frac{\partial U_2}{\partial t} &= D_2 \frac{\partial^2 U_2}{\partial x^2} - V_2 \frac{\partial U_2}{\partial x} + U_2(R_2(x) - A_{21}U_1 - A_{22}U_2), \end{aligned} \tag{2.1}$$

where $R_i(x)$ are the respective grow rates, A_{ij} are the interspecific and intraspecific competition coefficients, D_i are the diffusion coefficients, $V_1, V_2 > 0$ are spatially constant flow speeds. When we consider $K_j = \frac{R_j}{A_{ij}}$ as the carrying capacities, the reaction terms become

$$R_1 U_1 (1 - \frac{U_i + \alpha U_2}{K_1}),$$

where $\alpha = A_{12}/A_{11}$.

We take the model on a bounded domain $[0, L]$ where $x = 0$ is top of the river and downstream boundary will be at $x = L$. These assumptions can be combined under the Danckwerts [9] and Neumann boundary conditions:

$$D_i \frac{\partial U_i}{\partial x} - V_i U_i = 0, \quad x = 0\ ; \quad \frac{\partial U_i}{\partial x} = 0, \quad x = L, \quad i = 1, 2.$$

The boundary condition at $x = 0$ shows that individuals cannot cross the upstream boundary and move beyond the top of the stream. Moreover, the downstream condition shows that net out-flux from the domain because of the advection.

In [15], further simplifying assumption are introduced:

- Both species have the same diffusion and flow speeds, $D_1 = D_2 = D$, $V_1 = V_2 = V$.
- Growth rates are linear and non-decreasing, and $R_2/R_1 = \rho =$ constant, i.e, $R_1(x) = R_U + (R_L - R_U)x$, $R_U \leq R_L$, $R_2(x) = \rho R_1(x)$, where U ,L are the upper and lower end of the river section respectively.

For numerical simulations, we take the non-dimensional quantities

$$t' = t \max_x R_1(x) = tR_L, \quad x' = \frac{x}{L}, \quad d_i = \frac{D_i}{L^2 R_L}, \quad v_i = \frac{V_i}{LR_L}, \quad u_i = \frac{A_{ii}U_i}{R_L}.$$

Then the non-dimensional for is given as

$$\begin{aligned} \frac{\partial u_1}{\partial t} &= d_1 \frac{\partial^2 u_1}{\partial x^2} - v_1 \frac{\partial u_1}{\partial x} + u_1(r_1 - u_1 - a_{12}u_2), \\ \frac{\partial u_2}{\partial t} &= d_2 \frac{\partial^2 u_2}{\partial x^2} - v_2 \frac{\partial u_2}{\partial x} + u_2(r_2 - a_{21}u_1 - u_2), \end{aligned} \tag{2.2}$$

where $r_i = \frac{R_i(x)}{R_L}$ and $a_{ij} = \frac{A_{ij}}{A_{jj}}$.

2.2 Model:Three Competing Species Advective LV Model

Three competing species models show more diversity in population dynamics if it is compared with two competing species model, because there is no monotonicity in three dimensional systems in general [6]. Now, we consider the following advection-diffusion-reaction model for three competing species [30]

$$\begin{aligned}
\frac{\partial u_1}{\partial t} &= d\frac{\partial^2 u_1}{\partial x^2} - q\frac{\partial u_1}{\partial x} + u_1(r_1 - a_{11}u_1 - a_{12}u_2 - a_{13}u_3),\\
\frac{\partial u_2}{\partial t} &= d\frac{\partial^2 u_2}{\partial x^2} - q\frac{\partial u_2}{\partial x} + u_2(r_2 - a_{21}u_1 - a_{22}u_2 - a_{23}u_3),\\
\frac{\partial u_3}{\partial t} &= d\frac{\partial^2 u_3}{\partial x^2} - q\frac{\partial u_3}{\partial x} + u_3(r_3 - a_{31}u_1 - a_{32}u_2 - a_{33}u_3),
\end{aligned} \tag{2.3}$$

where $u_i(t,x)$ is the density of the i-th species at time t at point x of the bounded domain $[0,L]$. We suppose that the diffusion coefficient, $d > 0$, and the effective advection speed, $q \geq 0$, are the same for all three species. The intrinsic growth rates, r_i, and the inter- and intra-specific competition coefficients, a_{ij} are assumed to be positive. We impose again the same the boundary conditions as for the two species advective LV equations:

$$d\frac{\partial u_i}{\partial x}(t,0) - qu_i(t,0) = 0, \quad \frac{\partial u_i}{\partial x}(t,L) = 0.$$

As a result of this constraint, there are two possible arrangements between three competitors when the flow speed $q = 0$: i) cyclic case, ii) the transitive case.

In cyclic case $\lambda = 0$, λ is the leading eigenvalue of our model system. If growth rates of the species are in an order such that $r_1 > r_2 > r_3 > 0$, then two sub-cases of the cyclic case will occur. Species i outcompetes species $i-1$ (modulo 3) in one case, but in the other case species i outcompetes species $i+1$ (modulo 3). The parameters are taken as [30]

$$\begin{aligned}
a_{11} &= r_1, \quad a_{12} = \alpha r_1, \quad a_{13} = \beta r_1,\\
a_{21} &= \beta r_2, \quad a_{22} = r_2, \quad a_{23} = \alpha r_2,\\
a_{31} &= \alpha r_3, \quad a_{32} = \beta r_3, \quad a_{33} = r_3.
\end{aligned}$$

Then, the system 2.3 can be written as

$$\begin{aligned}
\frac{\partial u_1}{\partial t} &= r_1 u_1 \left((\left(1 + \frac{\lambda}{r_1}\right) - u_1 - \alpha u_2 - \beta u_3 \right),\\
\frac{\partial u_2}{\partial t} &= r_2 u_2 \left((\left(1 + \frac{\lambda}{r_2}\right) - \beta u_1 - u_2 - \alpha u_3 \right),\\
\frac{\partial u_3}{\partial t} &= r_3 u_3 \left(\left(1 + \frac{\lambda}{r_3}\right) - \alpha u_1 - \beta u_2 - u_3 \right),
\end{aligned}$$

where $0 < \beta < 1 < \alpha$ (case 1) or $0 < \alpha < 1 < \beta$ (case 2), and $\alpha\beta < 1$.

Persistency and permanence of these cases are studied also in [30]. Species 1 or species 3 is extinct for even smaller λ, so the system decreases to a two species system. The species with the highest growth rate will displace the other species.

In transitive case, species are ordered according to their competitive ability in which species 1 is the best competitor and species 3 is the worst competitor. Growth rates order is reverse of the cyclic case meaningly $0 < r_1 < r_2 < r_3$.

CHAPTER 3

DISCONTINUOUS GALERKIN METHOD

Discontinuous Galerkin methods were first proposed and analyzed in the early 1970s as a technique to numerically solve partial differential equations. In 1973, Reed and Hill [19] introduced a discontinuous Galerkin(DG) method to solve the hyperbolic neutron transport equation. Discontinuous Galerkin methods have been presented and studied for elliptic problems in [3, 22]and for convection diffusion problems in [5].

There are several advantages of DG methods. One of them is their flexibility with respect to mesh and local polynomial degree of the basis functions. As a result of this property, DG methods can be applied to complex domains by the use of unstructured grids or hanging nodes. Besides, different orders of approximations can be used with discretization on each element. The other advantages of DG methods is mass conservation on each mesh element and because of this property, DG methods can be a better choice to solve in flow and transport problems. The final advantage of DG methods is their compact formulation. Their compact formulation can be applied near boundaries without any special treatment. Hence, this increases the robustness and accuracy of any boundary condition implementation. Although there are several advantages of DG methods, the large number of degrees of freedom compared to standard finite element methods and ill conditioning of the matrices with increasing degree of the basis polynomials are disadvantages of DG methods.

In this chapter, we firstly give preliminaries, then one and two dimensional model problems with the general solution are given next parts. Finally, numerical example is given with the DG results.

3.1 Preliminaries

3.1.1 Function spaces

Let Ω denote a bounded polygonal domain in $\Omega \subset \mathbb{R}^d$. The vector space $L^2(\Omega)$ is the space of square-integrable functions:

$$L^2(\Omega) = \left\{ v \text{ measurable } : \int_\Omega v^2 < \infty \right\}.$$

The space $L^2(\Omega)$ is a Hilbert space with respect to the following inner product and norm

$$(u,v)_\Omega = \int_\Omega uv, \qquad ||v||_{L^2(\Omega)} = \left(\int_\Omega v^2\right)^{1/2}.$$

The space $L^\infty(\Omega)$ is the space of bounded functions

$$L^\infty(\Omega) = \left\{v : ||v||_{L^\infty(\Omega)} < \infty\right\}$$

equipped with the norm

$$||v||_{L^\infty(\Omega)} = \text{ess sup}\{|v(x)| : x \in \Omega\}.$$

Definition 3.1. Let $D(\Omega)$ denote the space of C^∞ functions with compact support in Ω. The dual space $D'(\Omega)$ is called the space of distributions. For any multi-index $\alpha = (\alpha_1, ..., \alpha_d) \in \mathbb{N}^d$ and $|\alpha| = \sum_{i=1}^d \alpha_i$, the distributional derivative $D^\alpha v \in D'(\Omega)$ is defined by

$$\forall \phi \in D(\Omega), \qquad D^\alpha v(\Omega) = (-1)^{|\alpha|} \int_\Omega v(x) \frac{\partial^{|\alpha|}\phi}{\partial x_1^{\alpha_1} ... \partial x_d^{\alpha_d}}.$$

For an integer s, then the Sobolev space is given by

$$H^s(\Omega) = \{v \in L^2(\Omega) : \forall 0 \le |\alpha| \le s,\ D^\alpha v \in L^2(\Omega)\}$$

equipped with the Sobolev norm and Sobolev seminorm, respectively

$$||v||_{H^s(\Omega)} = \left(\sum_{0 \le |\alpha| \le s} ||D^\alpha v||^2_{L^2(\Omega)}\right)^{\frac{1}{2}},$$

$$|v|_{H^s(\Omega)} = ||\nabla^s v||_{L^2(\Omega)} = \left(\sum_{|\alpha| = s} ||D^\alpha v||^2_{L^2(\Omega)}\right)^{\frac{1}{2}}.$$

For our special interest, we consider the following spaces

$$H^1(\Omega) = \left\{v \in L^2(\Omega) :\ \frac{\partial v}{\partial x_i} \in L^2(\Omega),\ i = 1, \cdots, d\right\},$$
$$H^1_0(\Omega) = \left\{v \in H^1(\Omega) :\ v|_{\partial\Omega} = 0\right\},$$
$$H^1_D(\Omega) = \left\{v \in H^1(\Omega) :\ v|_{\partial\Omega} = g_D\right\},$$

where g_D is a given Dirichlet boundary data.

Definition 3.2. Let V be a vector space. A symmetric bilinear form $a : V \times V \to \mathbb{R}$ is an inner product if $a(v,v) \ge 0$ for all $v \in V$ and $a(v,v) = 0$ if and only if $v = 0$. The space V is a normed space with the norm $||.||_v = (a(.,.))^{1/2}$. Moreover, the space V is equipped with an inner product is a Hilbert space if it is complete.

3.1.2 Trace theorems

Theorem 3.1. *Let Ω be a bounded domain with polygonal boundary $\partial\Omega$ and outward normal vector n. There exist trace operators $\gamma_0 : H^s(\Omega) \to H^{s-(1/2)}(\partial\Omega)$ for $s > 1/2$ and $\gamma_1 : H^s(\Omega) \to H^{s-(3/2)}(\partial\Omega)$ for $s > 3/2$ that are extensions of the boundary values and boundary normal derivatives, respectively. The operators γ_j are surjective. Furthermore, if $v \in C^1(\overline{\Omega})$, then*

$$\gamma_0 v = v|_{\partial\Omega}, \qquad \gamma_1 v = \nabla v \cdot n|_{\partial\Omega}.$$

Let $\mathbb{P}_k$ be the space of polynomials of degree less than or equal to k:

$$\mathbb{P}_k(E) = \text{span}\{x_1^{i_1} x_2^{i_2} ... x_d^{i_d} : i_1 + i_2 + ... + i_d \leq k, x \in E\},$$

where E is bounded polygonal domain with diameter h_E and $h_E = \sup_{x,y\in E}||x - y||$. The trace inequalities now become

$$\begin{aligned} &\forall v \in \mathbb{P}_k(E), \quad \forall e \in \partial E, \qquad ||v||_{L^2(e)} \leq \tilde{C}_t |e|^{-1/2} |E|^{-1/2} ||v||_{L^2(E)}, \\ &\forall v \in \mathbb{P}_k(E), \quad \forall e \in \partial E, \qquad ||v||_{L^2(e)} \leq C_t h_E^{-1/2} ||v||_{L^2(E)}. \end{aligned}$$

3.1.3 Green's Theorem

Given E a bounded domain and n_E the outward normal vector to ∂E, we have for all $v \in H^2(E)$ and $w \in H^1(E)$

$$-\int_E w \triangle v = \int_E \nabla v \cdot \nabla w - \int_{\partial E} \nabla v \cdot n_E w.$$

A more generalized Green's theorem is

$$-\int_E w \nabla \cdot F \nabla v = \int_E F \nabla v \cdot \nabla w - \int_{\partial E} F \nabla v \cdot n_E w,$$

where F is a matrix-valued function.

3.2 Construction of Discontinuous Galerkin Space Discretization

In this section, we give the detailed construction of discontinuous interior penalty Galerkin (IPG) methods, a type of discontinuous Galerkin (DG) methods, on 1D and 2D models. To do this, we just consider a simple Poisson problem. Using the Poisson equation as a starting point is meaningful since the DG methods concerns only with the diffusion parts of the PDEs.

3.2.1 Construction for 1D problems

Let us consider the general Poisson problem:

$$-\epsilon p'' = f(x), \qquad \forall x \in (0,1), \tag{3.1}$$

$$p(0) = g_0, \quad p(1) = g_1, \tag{3.2}$$

where $f \in C^0(0,1)$ and $p \in C^2(0,1)$ is the strong solution of the problem.

Consider the partition ξ_h:

$$0 = x_0 < x_1 < \ldots < x_N = 1,$$

$$I_n = (x_n, x_{n+1}) \ , \qquad h = x_{n+1} - x_n.$$

We set the space of piecewise discontinuous polynomials of degree k

$$V_h = \{v : v|_{I_n} \in P_k(I_n) \ \forall j = 0, 1, 2, ..., N-1\},$$

where P_k is the space of polynomials of degree at most k on the interval I_n. We need to define jump and average values of v since the functions in V_h are discontinuous at the interior nodes. The jump and average values of $v \in D_k(\xi_h)$ are given by

$$[v(x_n)] = v(x_n^-) - v(x_n^+), \quad \{v(x_n)\} = \frac{1}{2}(v(x_n^-) + v(x_n^+)),$$

where $v(x_n^-) = \lim_{x \to x_n^-} = v(x)$ and $v(x_n^+) = \lim_{x \to x_n^+} = v(x)$.

After multiplying the continuous Poisson equation (3.1) by a test function $v \in V_h$, and then applying integration by parts on each interval, we obtain for $n = 0, ..., N-1$

$$\int_{x_n}^{x_{n+1}} \epsilon p'(x)v'(x)dx - \epsilon p'(x_{n+1})v(x_{n+1}^-) + \epsilon p'(x_n)v(x_n^+) = \int_{x_n}^{x_{n+1}} f(x)v(x)dx.$$

For $1 \leq n \leq N-1$, there holds $[\epsilon p'(x_n)v(x_n)] = \{\epsilon p'(x_n)\}[v(x_n)] + \{v(x_n)\}[\epsilon p'(x_n)]$. Then, adding all N equations above and using the regularity assumption $[\epsilon p'(x_n)] = 0$ (p, p' are continuous), we get

$$\sum_{n=0}^{N-1} \int_{x_n}^{x_{n+1}} \epsilon p'(x)v'(x)dx - \sum_{n=0}^{N} \{\epsilon p'(x_n)\}[v(x_n)] = \int_0^1 f(x)v(x)dx.$$

Again using the regularity condition $[p(x_n)] = 0$, $1 \leq n \leq N-1$, we obtain,

$$\sum_{n=0}^{N-1} \int_{x_n}^{x_{n+1}} \epsilon p'(x)v'(x)dx - \sum_{n=0}^{N} \{\epsilon p'(x_n)\}[v(x_n)] + \kappa \sum_{n=1}^{N-1} \{\epsilon v'(x_n)\}[p(x_n)]$$
$$+ \sum_{n=1}^{N-1} \frac{\sigma_0}{h_{n-1,n}}[p(x_n)][v(x_n)] = \int_0^1 f(x)v(x)dx,$$

where σ_0 is a real non-negative number called the penalty parameter, and $\kappa \in \{-1, 0, 1\}$ is the parameter defining the IPG method. After adding boundary terms to the both sides, keeping unknown on the left side and imposing boundary conditions (3.2) on the right side, we obtain

$$\sum_{n=0}^{N-1} \int_{x_n}^{x_{n+1}} \epsilon p'(x)v'(x)dx - \sum_{n=0}^{N} \{\epsilon p'(x_n)\}[v(x_n)] + \kappa \sum_{n=0}^{N} \{\epsilon v'(x_n)\}[p(x_n)] + \sum_{n=0}^{N} \frac{\sigma_0}{h_{n-1,n}}[p(x_n)][v(x_n)] = \int_0^1 f(x)v(x)dx - g_0 \left(\kappa\epsilon v'(x_0) + \frac{\sigma^0}{h_{0,1}} v(x_0)\right) + g_1 \left(\kappa\epsilon v'(x_N) + \frac{\sigma^0}{h_{N-1,N}} v(x_N)\right).$$

Hence, for the diffusion part, we set the DG bilinear form $a_\kappa : V_h \times V_h \to \mathbb{R}$ by

$$a_\kappa(p, v) = \sum_{n=0}^{N-1} \int_{x_n}^{x_{n+1}} \epsilon p'(x)v'(x)dx - \sum_{n=0}^{N} \{\epsilon p'(x_n)\}[v(x_n)] + \kappa \sum_{n=0}^{N} \{\epsilon v'(x_n)\}[p(x_n)] + \sum_{n=0}^{N} \frac{\sigma_0}{h_{n-1,n}}[p(x_n)][v(x_n)]. \tag{3.3}$$

Then, solution of the Poisson equation (3.1) reads as: find $P^{DG} \in V_h$ such that

$$a_\kappa(P^{DG}, v) = L(v)\ , \qquad \forall v \in V_h$$

where the linear rhs $L : V_h \to \mathbb{R}$ is given by

$$L(v) = \int_0^1 f(x)v(x)dx - g_0 \left(\kappa\epsilon v'(x_0) + \frac{\sigma^0}{h_{0,1}} v(x_0)\right) + g_1 \left(\kappa\epsilon v'(x_N) + \frac{\sigma^0}{h_{N-1,N}} v(x_N)\right). \tag{3.4}$$

Depending on the parameter κ, several variations of DG methods are obtained.

- $\kappa = -1$: Symmetric interior penalty Galerkin (SIPG) method,
- $\kappa = +1$: Non-symmetric interior penalty Galerkin (NIPG) method,
- $\kappa = 0$: Incomplete interior penalty Galerkin(IIPG) method.

3.2.2 Construction for 2D problems

Let Ω be a polygonal domain in $\mathbb{R}^2$. Γ_D and Γ_N are two disjoint sets of sides of the boundary $\partial\Omega$. Let us take n as the unit normal vector to the boundary exterior to Ω. Consider the general Poisson equation

$$\begin{aligned} -\epsilon\Delta p &= f, && \text{in } \Omega, \\ p &= g_D, && \text{on } \Gamma, \end{aligned} \tag{3.5}$$

where $f \in L^2(\Omega)$ and $g_D \in H^{1/2}(\Gamma_D)$.

Let ξ_h be a partition of Ω including shape regular triangular elements E. Denote by Γ_h the set of interior edges and Γ_h^∂ the set of boundary edges. If two elements $E_1, E_2 \in \Gamma_h$ are neighbors and share one common side e, there are two traces of v along e. Thus, we set the jumps and averages on an interior edge by

$$[v] = (v|_{E_1}) - (v|_{E_2}), \quad \{v\} = \frac{1}{2}(v|_{E_1} + v|_{E_2}), \qquad \forall e = \partial E_1 \cap \partial E_2.$$

If $e \in \Gamma_h^\partial$, we set

$$[v] = v|_{E_1}, \quad \{v\} = v|_{E_1}, \qquad \forall e = \partial E_1 \cap \Gamma.$$

Following the same procedures and parameters in the construction of 1D DG scheme, solution of (3.5) reads as: find $P \in V_h = \{v \in L^2(\Omega) : v|_E \in P_k(\Omega),\ \forall E \in \xi_h\}$ such that

$$a_\kappa(P, v) = L(v), \quad \forall v \in V_h,$$

with

$$a_\kappa(P,v) = \sum_{E\in\xi_h}\int_E \epsilon\nabla P\cdot\nabla v - \sum_{e\in\Gamma_h\cup\Gamma_D}\int_e\{\epsilon\nabla P\cdot n_e\}[v] + \kappa\sum_{e\in\Gamma_h\cup\Gamma_D}\int_e\{\epsilon\nabla v\cdot n_e\}[P] + \sum_{e\in\Gamma_h\cup\Gamma_D}\int_e\frac{\sigma_e^0}{|e|}[P][v], \tag{3.6}$$

$$L(v) = \int_\Omega fv + \sum_{e\in\Gamma_D}\int_e\left(\kappa\epsilon\nabla v\cdot n_e + \frac{\sigma_e^0}{|e|}v\right)g_D, \tag{3.7}$$

where $|e|$ denotes the length of the edge e.

3.3 Implementation

In this section, we give a short description of the implementation tools of the DG schemes on 2D, which concerns with the evaluation of the volume and face integrals. To compute the integrals over every physical element in the mesh is too costly. Instead, the physical elements can be mapped to a reference elements.

Reference triangular element: It consists of a triangle $\widehat{E}$ with vertices $\widehat{A}_1(0,0)$, $\widehat{A}_2(1,0)$, $\widehat{A}_3(0,1)$. If E has vertices $A_i(x_i, y_i)$ for $i = 1, 2, 3$, then the map F_E is defined by

$$F_E\begin{pmatrix}\widehat{x}\\ \widehat{y}\end{pmatrix} = \begin{pmatrix}x\\ y\end{pmatrix}, \qquad x = \sum_{i=1}^3 x_i\widehat{\psi}_i(\widehat{x},\widehat{y}), \quad y = \sum_{i=1}^3 y_i\widehat{\psi}_i(\widehat{x},\widehat{y})$$

with

$$\widehat{\psi}_1(\widehat{x},\widehat{y}) = 1 - \widehat{x} - \widehat{y}, \quad \widehat{\psi}_2(\widehat{x},\widehat{y}) = \widehat{x}, \quad \widehat{\psi}_3(\widehat{x},\widehat{y}) = \widehat{y}.$$

Rewriting the mapping

$$\begin{pmatrix} x \\ y \end{pmatrix} = F_E \begin{pmatrix} \widehat{x} \\ \widehat{y} \end{pmatrix} = B_E \begin{pmatrix} \widehat{x} \\ \widehat{y} \end{pmatrix} + b_E,$$

where

$$B_E = \begin{pmatrix} x_2 - x_1 & x_3 - x_1 \\ y_2 - y_1 & y_3 - y_1 \end{pmatrix}, \qquad b_E = \begin{pmatrix} x_1 \\ y_1 \end{pmatrix}.$$

Basic functions: DG basis functions are set to be the functions spanning the DG space

$$V_h = \text{span}\{\varphi_i^E : 1 \le i \le N_{loc}, E \in \xi_h\}$$

with

$$\varphi_i^E(x) = \begin{cases} \widehat{\varphi}_i \circ F_E(x), & x \in E, \\ 0, & x \neq E, \end{cases}$$

where the local basis functions $(\widehat{\varphi}_i)_{1\le i\le N_{loc}}$ are defined on the reference element only. For 2D, for instance, we may choose the monomial basis functions

$$\widehat{\varphi}_i(\widehat{x},\widehat{y}) = \widehat{x}^I \widehat{y}^J, \quad I + J = i, \quad 0 \le i \le k$$

with the local dimension $N_{loc} = \frac{(k+1)(k+2)}{2}$. Then, the DG solution has the form

$$p(x) = \sum_{j=1}^{N_{El}} \sum_{i=1}^{N_{loc}} U_i^j \varphi_i^{E_j}(x) \,, \qquad U_i^j \in \mathbb{R},$$

where U_i^j's denote the unknown coefficients.

Reference to Global:

The mapping $F_E : \widehat{E} \mapsto E$ corresponds to a change of variable. Denote $\widehat{v} = v \circ F_E$. Then we can write

$$\widehat{\nabla}\widehat{v} = B_E^T \nabla v \circ F_E.$$

Hence,

$$\int_E v = 2|E| \int_{\widehat{E}} \widehat{v},$$

$$\int_E \nabla v \cdot u = 2|E| \int_{\widehat{E}} (B_E^T)^{-1} \widehat{\nabla}\widehat{v} \cdot \widehat{y},$$

$$\int_E \nabla v \cdot \nabla u = 2|E| \int_{\widehat{E}} (B_E^T)^{-1} \widehat{\nabla}\widehat{v} \cdot (B_E^T)^{-1} \widehat{\nabla}\widehat{y}.$$

Implementation (volume contribution): There are two types of local matrices depending on the domain of integration. First, compute the matrix A_E resulting from the volume integral of the diffusion part over a fixed element E. $\forall 1 \le i,j \le N_{loc}$,

$$(A_E)_{i,j} = \int_E \nabla\varphi_{i,E} \cdot \nabla\varphi_{j,E} = 2|E| \int_{\widehat{E}} (B_E^T)^{-1} \widehat{\nabla}\widehat{\varphi}_i \cdot (B_E^T)^{-1} \widehat{\nabla}\widehat{\varphi}_j,$$

and the local right-hand side b_E

$$(b_E)_i = \int_E f\varphi_{i,E} = 2|E| \int_{\widehat{E}} \widehat{f}\widehat{\varphi}_{i,E}.$$

Implementation (face contribution): Secondly, compute the local matrices corresponding to the integrals over a fixed face e. If $e \in \Gamma_h$, the terms involving integrals on e are

$$T = -\int_e \{\nabla p\}[v] + \kappa \int_e \{\nabla v\}[p] + \frac{\sigma}{|e|}\int_e [p][v].$$

Expanding the averages and jumps, we obtain

$$T = M_e^{1,1} + M_e^{2,2} + M_e^{1,2} + M_e^{2,1}$$

with

$$(M_e^{p,r})_{i,j} = (-1)^p \frac{1}{2}\int_e \nabla\varphi_{j,E_e^r}\varphi_{i,E_e^p} + (-1)^{r+1}\frac{\kappa}{2}\int_e \nabla\varphi_{i,E_e^p}\varphi_{j,E_e^r}$$

$$+(-1)^{p+r}\frac{\sigma}{|e|}\int_e \varphi_{j,E_e^r}\varphi_{i,E_e^p} \qquad 1 \le i,j \le N_{loc}, 1 \le p,r \le 2.$$

If $e \in \Gamma$, we only compute

$$(M_e^{1,1})_{i,j} = -\int_e \nabla\varphi_{j,E_e^1}\varphi_{i,E_e^1} + \kappa\int_e \nabla\varphi_{i,E_e^1}\varphi_{j,E_e^1} + \frac{\sigma}{|e|}\int_e \varphi_{j,E_e^1}\varphi_{i,E_e^1}$$

and

$$(b_e)_i = \int_e \left(\kappa\nabla\varphi_{i,E_e^1} + \frac{\sigma}{|e|}\varphi_{i,E_e^1}\right) g.$$

CHAPTER 4

TIME DISCRETIZATION

In this chapter, we deal with the time integrators used in this thesis in order to discretize the model equation (1.1) in time. We discuss mainly the following time integrators: the first order backward Euler and the second order IMEX methods. For convenient, we just consider the scalar form of the model equation (1.1) given by

$$\frac{\partial u}{\partial t} + v \cdot \nabla u - d\Delta u + R(u) = f(x,t), \quad \text{on } \Omega \times J, \tag{4.1}$$

where $J = (0,T)$ and Ω is a bounded domain in $\mathbb{R}^1$ or $\mathbb{R}^2$ with a smooth or piecewise boundary, and with appropriate boundary conditions. The classical weak formulation of (4.1) reads as: for a.e. $t \in J$, for any $w \in H_0^1(\Omega)$, find $u \in L^2(0,T;H_0^1(\Omega)) \cap H^1(0,T;L^2(\Omega))$ such that

$$\int_\Omega \frac{\partial u}{\partial t} w dx + a(t;u,w) + b(t;u,w) = l(w), \tag{4.2}$$

$$\begin{aligned} a(t;u,w) &= \int_\Omega (d\nabla u(t) \cdot \nabla w + v \cdot \nabla u(t) w) dx, \\ b(t;u,w) &= \int_\Omega R(u(t)) w dx, \\ l(w) &= \int_\Omega f w dx. \end{aligned}$$

It is well-known that under certain conditions, the system (4.2) has a unique solution. On the other hand, using the notations and definitions given in Chapter 3, the semi-discrete DG formulation of the model (4.1) reads as: for a.e. $t \in J$, find $u_h \in C^{0,1}(0,T;V_h)$ such that

$$\int_\Omega \frac{\partial u_h}{\partial t} w_h dx + \tilde{a}_h(t;u_h,w_h) + b_h(t;u_h,w_h) = l(w_h) \tag{4.3}$$

with

$$\begin{aligned} \tilde{a}_h(t;u_h,w_h) &= a_h(t;u_h,w_h) + \sum_{E \in \xi_h} \int_E v \cdot \nabla u_h w_h dx, \\ b_h(t;u_h,w_h) &= \sum_{E \in \xi_h} \int_E R(u_h) w_h dx. \end{aligned}$$

In (4.3), the component $a_h(t; u_h, w_h)$ of the bilinear form $\tilde{a}_h(t; u_h, w_h)$ and the linear rhs $l(w_h)$ are defined by (3.3) and (3.4), respectively, for 1D model or by (3.6) and (3.7), respectively, for 2D model, at a given time instance $t \in J$ and for a choice of the DG parameter $\kappa \in \{-1, 0, 1\}$. The semi-discrete system (4.3) leads to the system of non-linear equations in matrix-vector form by

$$M\mathbf{U}_t + S\mathbf{U} = \mathbf{L} - \mathbf{b}(\mathbf{U}), \tag{4.4}$$

where $\mathbf{U}$ is the vector of unknown coefficients, the matrix S is the stiffness matrix related to the bilinear form $\tilde{a}_h(t; u_h, v_h)$, and the vector function $\mathbf{b}(\mathbf{U})$ and the vector $\mathbf{L}$ corresponds to the non-linear form $b_h(t; u_h, v_h)$ and the linear form $l_h(v_h)$, respectively, the explicit forms of which will be given later. The matrix M is the usual mass matrix which by DG construction has a symmetric block diagonal structure, and therefore it is a symmetric positive definite matrix. As a consequent, in the algebraic point of view, what we have in the ODE system (4.4) is that M is an invertible matrix, S is a positive definite matrix and the right hand side is Lipschitz with respect to $\mathbf{U}$, which means by the theory of ordinary differential equations that the system (4.4), as a result, the semi-discrete problem (4.3) has a unique solution.

4.1 Fully Discrete Formulations

In this section, we derive the fully discrete formulations of the system (4.3) by using the time integrators used in this thesis. We divide $J = [0, T]$ into n pieces such that $\Delta t = T/n$ shows the length of interval and $t^{n+1} = t^n + \Delta t$ for all $n \geq 0$. Let ξ_h^n be the mesh related to the n^{th} time step. We take finite element space as $V_h^n = V_h(\xi_h^n)$ related to each time step.

4.1.1 Backward Euler Discretization

First, we discuss the the fully discrete formulation of the system (4.3) by first order backward Euler method. We consider an arbitrary k^{th} time-step, which is solved for all $k = 1, 2, \ldots, n$. In order to not be confused about the notations, let us consider the backward Euler fully discrete formulation of the system (4.3) on an arbitrary k^{th} time-step without the superscript for the time-step of the form

$$\int_\Omega \frac{u_h - w_h}{\Delta t} v_h dx + \tilde{a}_h(u_h, v_h) + b_h(u_h, v_h) = l(v_h) \ , \quad \forall v_h \in V_h \tag{4.5}$$

where we have set $u_h := u_h^k$, $w_h := u_h^{k-1}$, $v_h := v_h^k$, $\Delta t := \Delta t_k$, $\tilde{a}_h(u_h, v_h) := \tilde{a}_h(t^k; u_h^k, v_h^k)$, $b_h(u_h, v_h) := b_h(t^k; u_h^k, v_h^k)$ and $V_h := V_h^k$. The approximate solution u_h and the known solution (from the previous time-step) w_h of (4.5) have the form

$$u_h = \sum_{i=1}^{Nel} \sum_{l=1}^{Nloc} u_l^i \phi_l^i \ , \quad w_h = \sum_{i=1}^{Nel} \sum_{l=1}^{Nloc} w_l^i \phi_l^i, \tag{4.6}$$

where ϕ_l^i's are the basis polynomials spanning the space V_h, $\mathbf{U} = \{u_l^i\}$ is the vector of unknown coefficients to be found and $\mathbf{W} = \{w_l^i\}$ is the vector of known coefficients. Then, the discrete residual of the system (4.5) in matrix-vector form is given by

$$Res(\mathbf{U}) = M\mathbf{U} - M\mathbf{W} + \Delta t(S\mathbf{U} + \mathbf{b}(\mathbf{U}) - \mathbf{L}) = 0, \tag{4.7}$$

where M is the mass matrix, S is the stiffness matrix corresponding to the bilinear form $\tilde{a}_h(u_h, v_h)$, $\mathbf{b}(\mathbf{U})$ is the vector function of $\mathbf{U}$ related to the non-linear form $b_h(u_h, v_h)$ and $\mathbf{L}$ is the vector to the linear form $l_h(v_h)$.

Next, we solve the system (4.7) by Newton method. In the sequel, we start with an initial guess $\mathbf{U}^{(0)}$ (most possibly $\mathbf{U}^{(0)} = \mathbf{W}$, i.e. the known solution from the previous time-step) and for $i = 0, 1, 2, \ldots$, we solve the system

$$\begin{aligned} J^i \delta\mathbf{U}^{(i)} &= -Res(\mathbf{U}^{(i)}) \\ \mathbf{U}^{(i+1)} &= \mathbf{U}^{(i)} + \delta\mathbf{U}^{(i)} \end{aligned} \tag{4.8}$$

until a prescribed tolerance is satisfied. In (4.8), the sparse matrix $J^i = M + \Delta t(S + J^i_{\mathbf{b}})$ denotes the value of the Jacobian matrix of the residual function $Res(\mathbf{U})$ at the current iterate $\mathbf{U}^{(i)}$, and $J^i_{\mathbf{b}}$ stands for the Jacobian matrix to the vector function $\mathbf{b}(\mathbf{U})$ at the current iterate $\mathbf{U}^{(i)}$.

For the explicit definitions of the matrices and vectors, firstly we give block matrices which have $Nloc$ dimension:

$$M_{ij} = \begin{bmatrix} \int_\Omega \phi_1^i \phi_1^j dx & \int_\Omega \phi_2^i \phi_1^j dx & \cdots & \int_\Omega \phi_{Nloc}^i \phi_1^j dx \\ \int_\Omega \phi_1^i \phi_2^j dx & \int_\Omega \phi_2^i \phi_2^j dx & \cdots & \vdots \\ \vdots & \ddots & \ddots & \vdots \\ \int_\Omega \phi_1^i \phi_{Nloc}^j dx & \cdots & \cdots & \int_\Omega \phi_{Nloc}^i \phi_{Nloc}^j dx \end{bmatrix}$$

$$S_{ij} = \begin{bmatrix} \tilde{a_h}(\phi_1^i \phi_1^j) & \tilde{a_h}(\phi_2^i \phi_1^j) & \cdots & \tilde{a_h}(\phi_{Nloc}^i \phi_1^j) \\ \tilde{a_h}(\phi_1^i \phi_2^j) & \tilde{a_h}(\phi_2^i \phi_2^j) & \cdots & \vdots \\ \vdots & \ddots & \ddots & \vdots \\ \tilde{a_h}(\phi_1^i \phi_{Nloc}^j) & \cdots & \cdots & \tilde{a_h}(\phi_{Nloc}^i \phi_{Nloc}^j) \end{bmatrix}$$

$$\mathbf{b}_i(\mathbf{U}) = \begin{bmatrix} b_h(u_h, \phi_1^i) \\ b_h(u_h, \phi_2^i) \\ \vdots \\ b_h(u_h, \phi_{Nloc}^i) \end{bmatrix}, \qquad \mathbf{L}_i = \begin{bmatrix} l(\phi_1^i) \\ l(\phi_2^i) \\ \vdots \\ l(\phi_{Nloc}^i) \end{bmatrix}.$$

Now, the explicit definitions are

$$S = \begin{bmatrix} S_{11} & S_{12} & \cdots & S_{1,Nel} \\ S_{21} & S_{22} & \cdots & \vdots \\ \vdots & \ddots & \ddots & \vdots \\ S_{Nel,1} & \cdots & \cdots & S_{Nel,Nel} \end{bmatrix}, \qquad M = \begin{bmatrix} M_{11} & M_{12} & \cdots & M_{1,Nel} \\ M_{21} & M_{22} & \cdots & \vdots \\ \vdots & \ddots & \ddots & \vdots \\ M_{Nel,1} & \cdots & \cdots & M_{Nel,Nel} \end{bmatrix}$$

$$\mathbf{b}(\mathbf{U}) = \begin{bmatrix} \mathbf{b}_1(\mathbf{U}) \\ \mathbf{b}_2(\mathbf{U}) \\ \vdots \\ \mathbf{b}_{Nel}(\mathbf{U}) \end{bmatrix}, \qquad \mathbf{L} = \begin{bmatrix} \mathbf{L}_1 \\ \mathbf{L}_2 \\ \vdots \\ \mathbf{L}_{Nel} \end{bmatrix}.$$

4.1.2 IMEX Method

In this section, we give a semi-implicit time discretization method which belongs to the class of implicit-explicit IMEX methods [4]. Linear multi-step IMEX schemes have been used frequently for the integration of nonlinear ordinary differential equations arising from discretization of PDEs. In case of semi-linear ADR equation, the linear diffusion and advection terms are integrated implicitly and the nonlinear term explicitly. The resulting scheme require only the solution of a linear system of equations at each time step in contrast to the fully implicit methods like the backward Euler method, which requires solution of nonlinear system of equation at each time step. Due to the semi-implicit nature, the IMEX methods have step-size restrictions due the stability of the numerical scheme. For the integration of the (in matrix-vector form) semi-discrete ADR equation 4.4, we have chosen the two step IMEX-BDF (backward differentiation) method in [1] leading for $k = 0, 1, \ldots, n-2$ to the system

$$M\left(\frac{3}{2}U^{k+2} - 2U^{k+1} + \frac{1}{2}U^{k}\right) + \Delta t S U^{k+2} = \Delta t\left(\mathbf{b}(\mathbf{U}^{k}) - \mathbf{L}^{k}\right) - 2\Delta t\left(\mathbf{b}(\mathbf{U}^{k+1}) - \mathbf{L}^{k+1}\right),$$

where the superscript k denotes the related value at the $k-th$ time instance. The above IMEX-BDF method is started after the computation of the value U^1 by the backward Euler method.

CHAPTER 5

NUMERICAL SIMULATIONS

In this section, we analyzed three examples of advection-reaction-diffusion(ADR) models from two different application areas. One of them is evolution of the two-stage competitive-consecutive, reaction-response problem which belongs to chemical species in a fluid. The other ones are evolution densities of two and three competing species in river ecosystems. We present convergence rates of the three different interior penalty Galerkin ($\kappa \in \{-1, 0, 1\}$) discretization for a four species ADR equation in [13] with the implicit Euler method and the semi-implicit IMEX-BDF method. Numerical solutions of two and three species advective Lotka-Volterra equations in Chapter 2 are given by symmetric interior penalty discontinuous Galerkin discretization (SIPG, $\kappa = -1$). In all numerical examples we have taken the penalization parameter as $\sigma = 10$.

5.1 Solution of a Nonlinear System by DG Method

We consider the ADR equation (1.1) in a unit disk $\Omega = \{(x, y)|x^2 + y^2 = 1\}$ [13] with 4 components (m=4). This is a reaction-response model of chemical species in a fluid. The nonlinear reaction terms are the linear combinations of the products of the components given by

$$\begin{aligned}
R_1(u_1, \ldots, u_4) &= k_1 u_1 u_2, \\
R_2(u_1, \ldots, u_4) &= k_1 u_1 u_2 + k_2 u_2 u_3, \\
R_3(u_1, \ldots, u_4) &= -k_1 u_1 u_2 + k_2 u_2 u_3, \\
R_4(u_1, \ldots, u_4) &= -k_2 u_2 u_3
\end{aligned}$$

where the parameters $k_1 = 100$ and $k_2 = 1$. The force functions f_i's, $i = 1, \ldots, 4$, and the Dirichlet boundary conditions are chosen with the exact solutions

$$\begin{aligned}
u_1 &= (r_0^2 - x^2 - y^2)(1 + x^2)(1 + t), \\
u_2 &= (r_0^2 - x^2 - y^2)(x^2 + y^2)(1 + \cos(t)), \\
u_3 &= (r_0^2 - x^2 - y^2)(1 + \cos(y))(1 - \sin(t)), \\
u_4 &= (r_0^2 - x^2 - y^2)(2 + x^2 + y^2)t,
\end{aligned}$$

The constants k_1 and k_2 are the reaction rates, u_1 and u_2 are the reactants, u_3 is the desired product and u_4 the waste, which is initially zero. The diffusion constant d is taken as 1, and the two dimensional flow rates are taken as $v = (v_1, v_2) = (1, 1)$.

In the Figures 5.1-5.4, convergence rates for three different DG methods for backward Euler and IMEX-BDF time discretizations are given. $\Delta x = 0.2102$ and $\Delta t = 0.005$ at the final time $t = 1$ are taken to solve this model. Three figures at the top are obtained by backward Euler and three figures at he bottom are obtained by IMEX-BDF method. Moreover, left side figures are solved by IIPG method, right side figures are solved by NIPG method and finally figures in the middle are solved by SIPG method in space. With an increasing degree in the DG approximation, the errors decrease. For degree 1 and 2, the convergence rates are about 2. The slope of lines give insight about these convergence rates. For degree 3, Figures 5.1-5.4 do not indicate any improvement after certain degree of freedom. The results of both time discretization methods are same. The problem is solved without using very small time steps.

The numerical solutions and error plots for the SIPG discretization with $\Delta x = 0.2102$ and $\Delta t = 0.005$ at the final time $t = 1$ are given in Figures 5.5-5.8. Top two figures belong to backward Euler method and bottom two figures belong to IMEX-BDF method. Figures show that results of both methods are the same and numerical solutions approach to exact solutions. This result can be understood from the error plots.

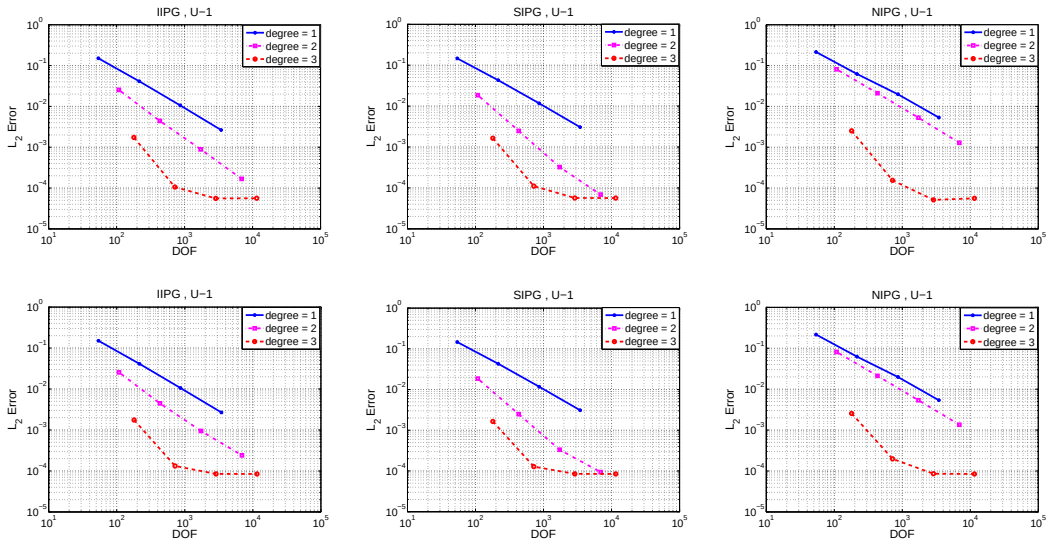

Figure 5.1: Numerical errors for u_1 with backward Euler (top) and IMEX-BDF scheme (bottom)

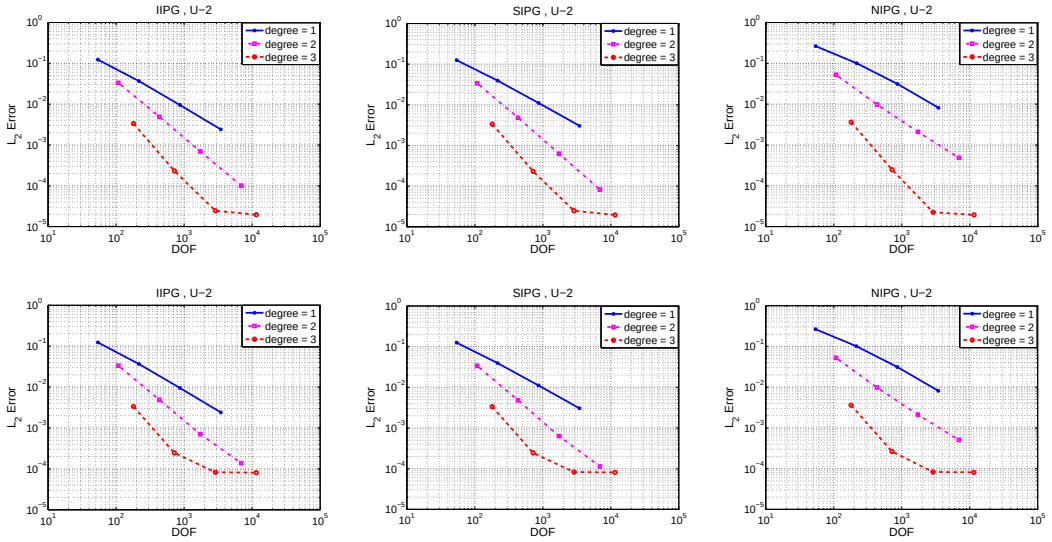

Figure 5.2: Numerical errors for u_2 with backward Euler (top) and IMEX-BDF scheme (bottom)

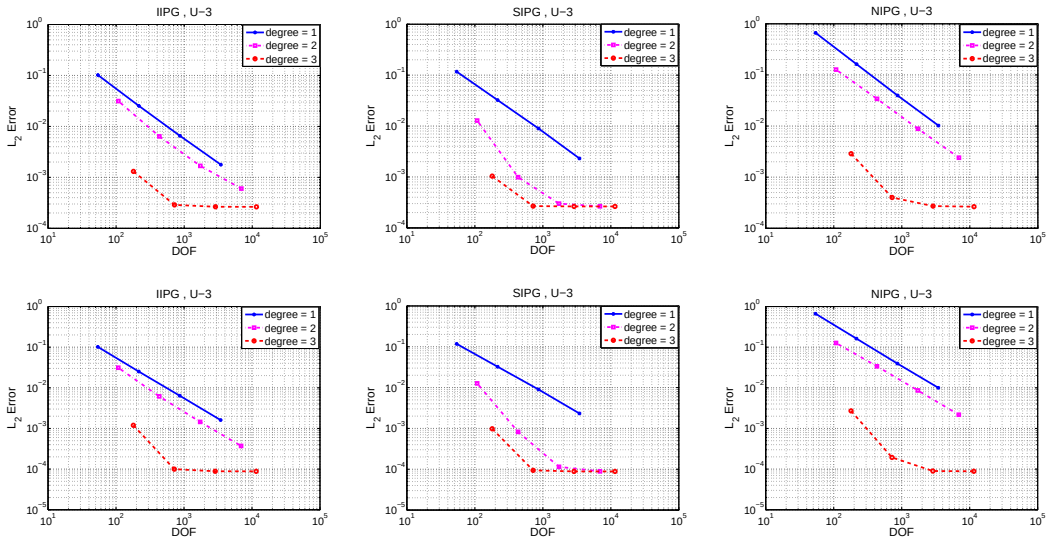

Figure 5.3: Numerical errors for u_3 with backward Euler (top) and IMEX-BDF scheme (bottom)

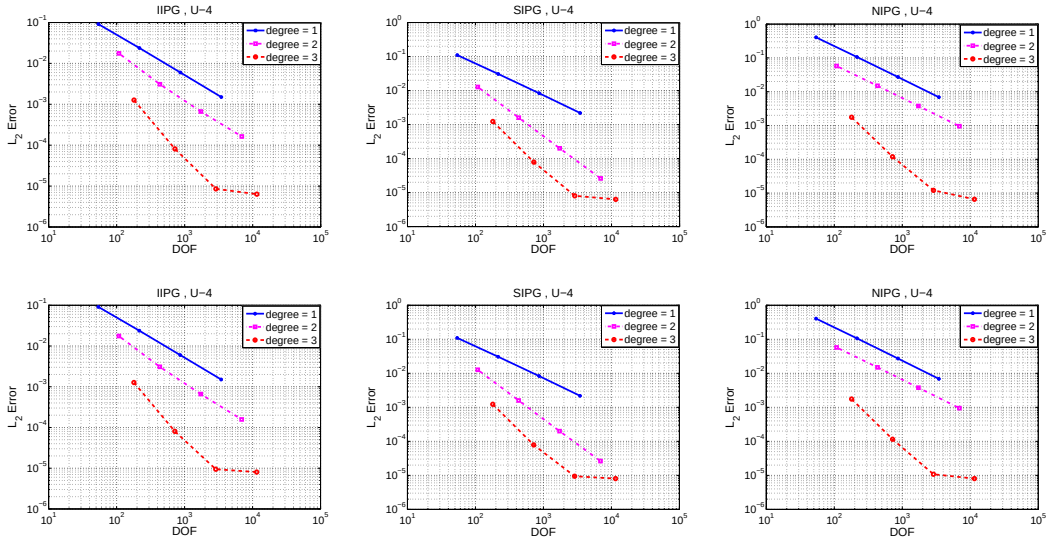

Figure 5.4: Numerical errors for u_4 with backward Euler (top) and IMEX-BDF scheme (bottom)

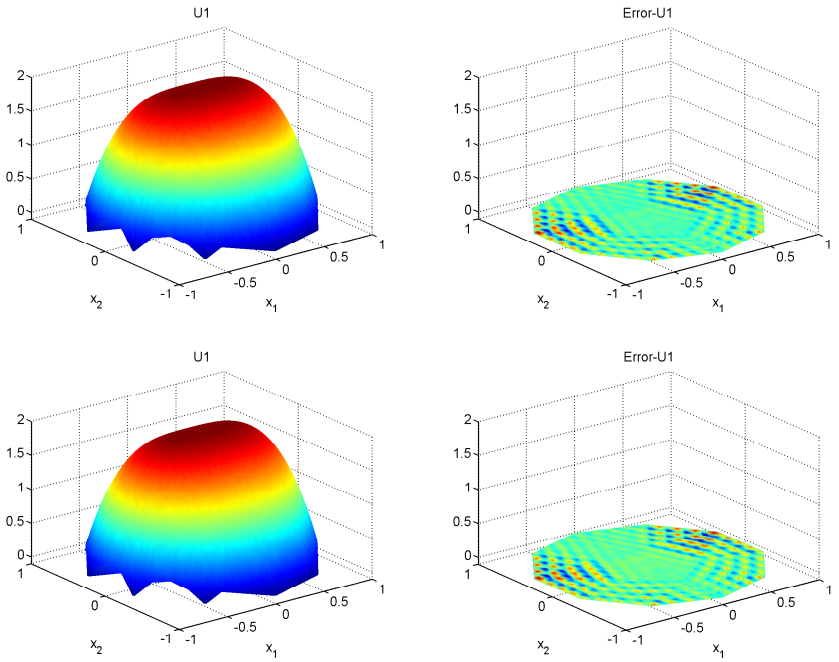

Figure 5.5: Numerical solution (left) and error plot (right) for u_1 at the final time using backward Euler (top) and IMEX-BDF scheme (bottom)

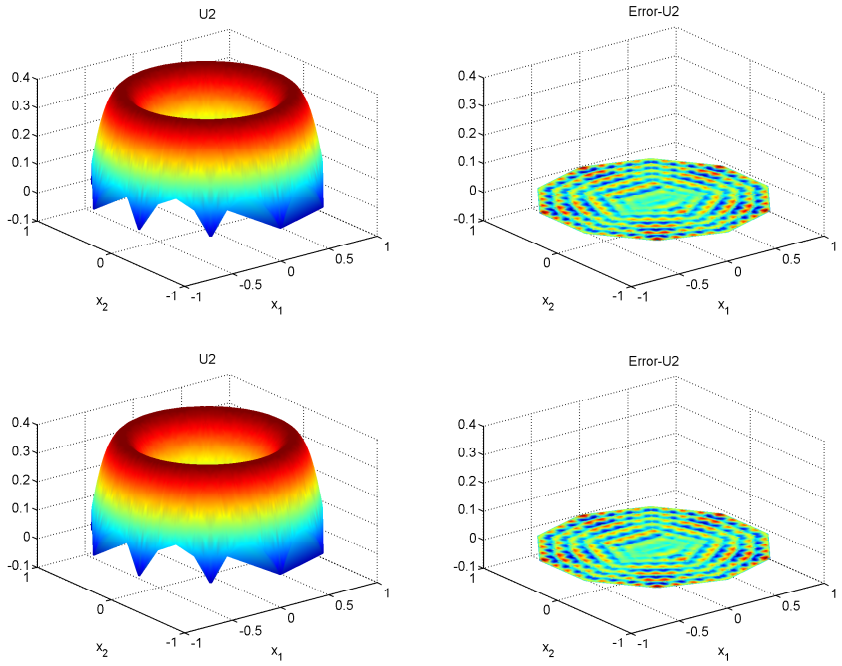

Figure 5.6: Numerical solution (left) and error plot (right) for u_2 at the final time using backward Euler (top) and IMEX-BDF scheme (bottom)

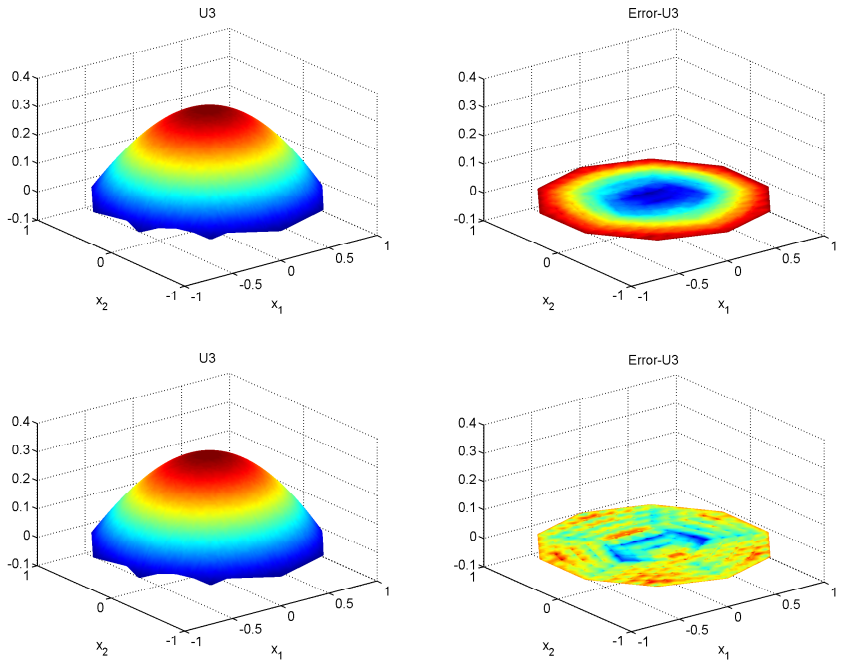

Figure 5.7: Numerical solution (left) and error plot (right) for u_3 at the final time using backward Euler (top) and IMEX-BDF scheme (bottom)

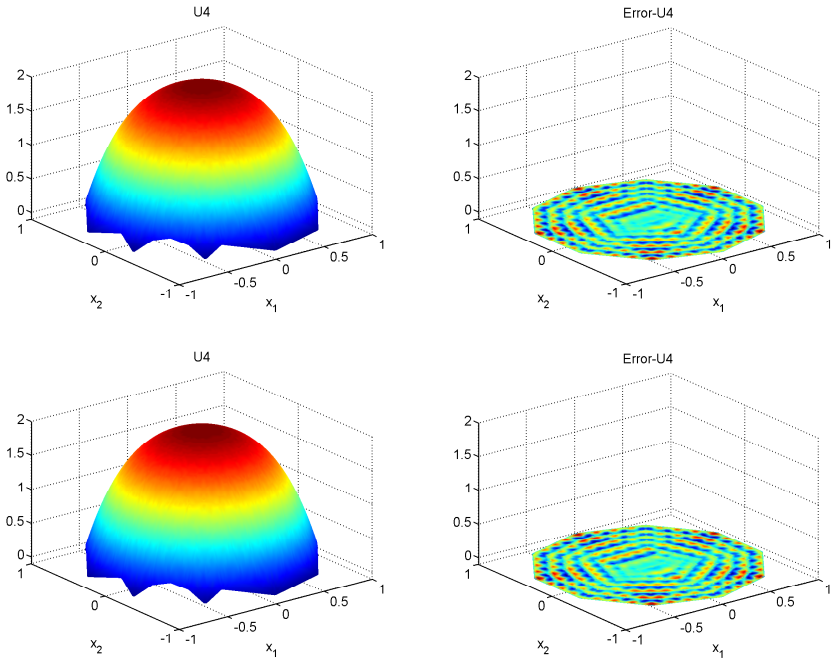

Figure 5.8: Numerical solution (left) and error plot (right) for u_4 at the final time using backward Euler (top) and IMEX-BDF scheme (bottom)

5.2 Solution of a Lotka-Volterra System with Two Competing Species

The advective Lotka-Volterra system (2.1) with two computing species in river ecosystem is solved by SIPG. Here $U_1 and U_2$ are the densities. Densities are the concentrations of species on a particular area of the river. The parameters are taken as in [15]:

$$L = 100, D = 1, R_U = R_L = 1, \rho = 1.4, V = 1.2,$$

$$A_{11} = A_{22} = 1, A_{12} = 0.5, A_{21} = 1.5.$$

The diffusion constants and flow rates are $D = (D_1, D_2) = (1, 1), V = (V_1, V_2) = (1.2, 1.2)$. Since $R_1(x) = R_U + (R_L - R_U)x$ and $R_2(x) = \rho R_1(x)$, it follows that $R_1 = 1$ and $R_2 = 1.4$, respectively. Here R_U shows the growth rate at the top and R_L is the growth rate at the downstream of the river. We used Danckwerts boundary conditions, so top of the river is $x = 0$ and downstream of the river is $X = L$. For space and time discretization we have taken $\Delta x = 0.5$ and $\Delta t = 0.01$.

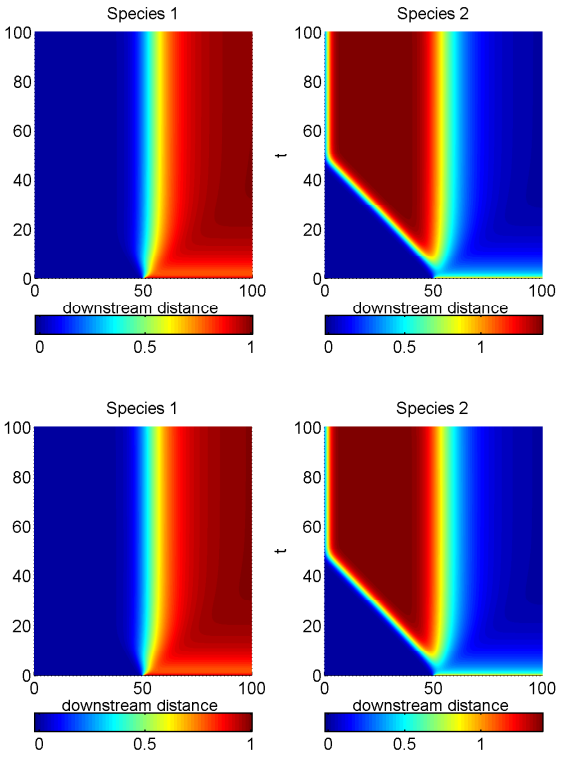

Figure 5.9: Evolution of densities of two competing species solved by implicit Euler (top) and IMEX-BDF scheme (bottom)

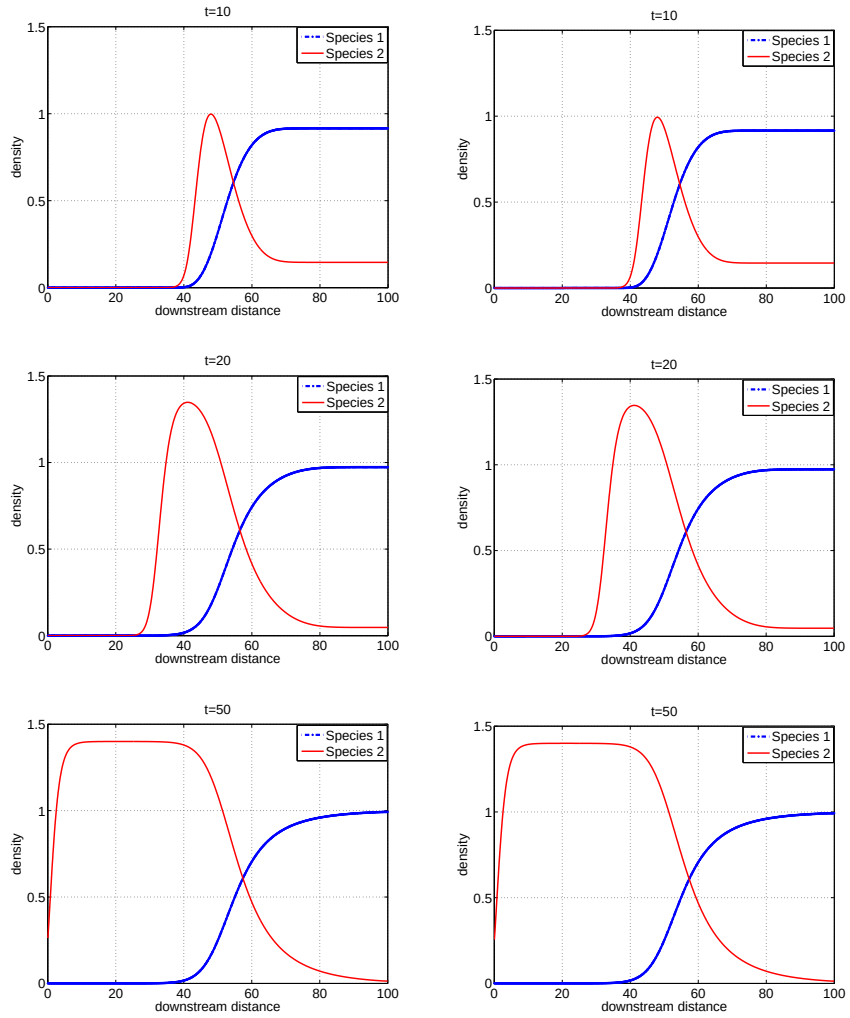

Figure 5.10: Densities of two competing species solved by implicit Euler (left) and IMEX-BDF scheme (right)

Lutscher [15] solved this problem by using numerical methods which are backward Euler method in time, finite difference method in space for the diffusion term and upwind for the advection term, however we solved this problem by using SIPG in space and by using fully implicit Euler method and semi-implicit IMEX-BDF method in time. Figure 5.9-5.10 show the evolution of densities at different time levels. Left side figures are obtained by using backward Euler method and the figures on the right side are obtained by IMEX-BDF method. Numerical results for both time discretizations are similar. A semi-implicit method which is more efficient than fully implicit methods gave the same result without using smaller time steps. As in [15] after a short time, densities of both species decrease upstream. The species 2 shows much more decrease than the species 1 at t=10. When time passes, species 1 catches its initial density in the upstream and species 2 is out of compete. We observe that a coexistence place between species occurs.

5.3 Solution of a Lotka-Volterra System with Three Competing Species

In this section, we have solved the system (2.3) which consists of three competing species in river ecosystem by using SIPG method in space. In this example, we have taken the parameters as:

$$
\begin{aligned}
&L = 100, D = 1, \rho = 1.4, V = 0.8,\\
&r_1 = 1.6, r_2 = 1.3, r_3 = 1,\\
&A_{11} = 1.6, A_{22} = 1.3, A_{33} = 1,\\
&A_{12} = 1.6, A_{21} = 0.65, A_{13} = 0.5,\\
&A_{31} = 1.6, A_{23} = 2.08, A_{32} = 0.5.
\end{aligned}
$$

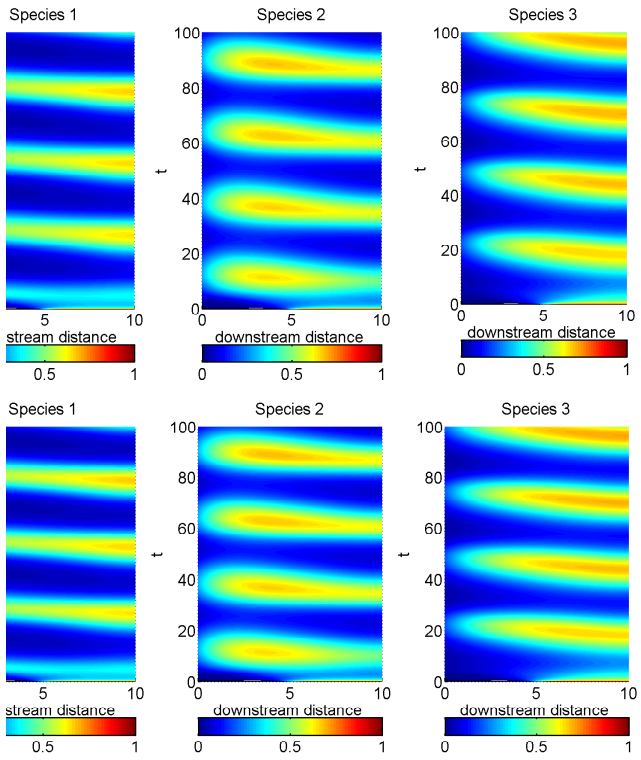

Figure 5.11: Evolution of densities of three competing species solved by implicit Euler (top) and IMEX-BDF scheme (bottom)

In Figure 5.11-5.12, we show the evolution of the three species' densities and the three species' densities at certain times, respectively, for fully implicit Euler and semi-implicit IMEX-BDF schemes for $\Delta x = 0.5$ and $\Delta t = 0.01$.

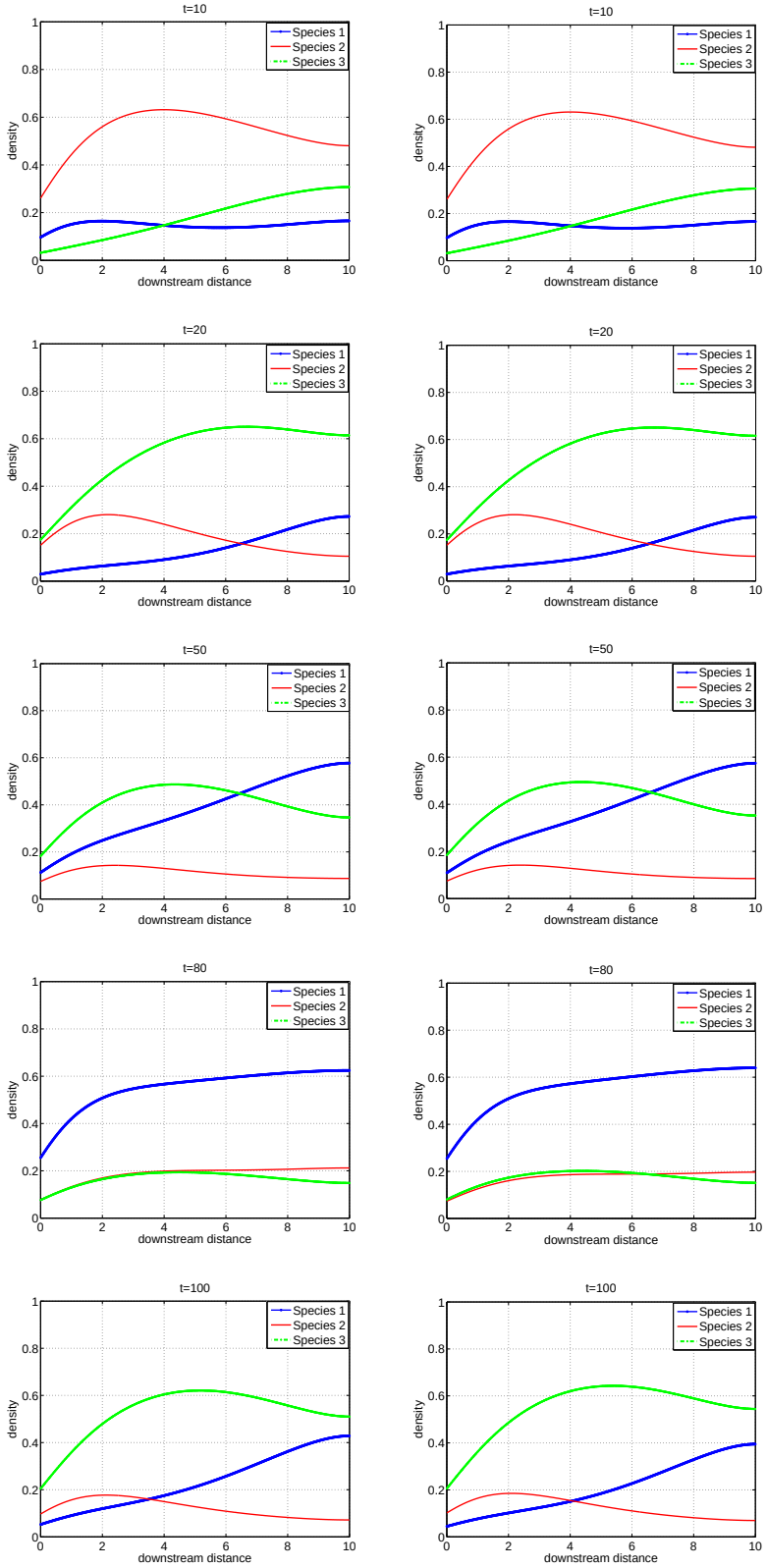

Figure 5.12: Densities of three competing species solved by implicit Euler (left) and IMEX-BDF scheme (right)

Left side figures are obtained by using fully implicit backward Euler and right side figures are obtained by using semi-implicit IMEX-BDF method in time. Numerical results are same as in the two competing species advective LV model example. Decreases in the densities are seen for all species towards to the upstream after a short time. The reason, especially for species 2 and species 3, is the invasion to the downstream. The invasion speed of species 2 is faster than species 3 at the beginning. The density of species 2 decreases at the downstream when the density of species 3 increases at this part of the domain. Then, species 1 starts to move towards downstream slowly. There are time levels which coexistence between species occurs. After a while, each species catch their own balance densities.

CHAPTER 6

CONCLUSIONS

In this thesis we have integrated ADR equations from chemical kinetics and advective Lota-Volterra equations in river systems. We have analyzed three examples which are competitive-consecutive, reaction-response of four chemical species in a fluid, two competing species advective LV model and three competing species advective LV model to compare a fully implicit method backward Euler and semi-implicit method IMEX-BDF. In space, DG construction is applied to these problems. We have discretized space and obtained a global system from the local construction. Then time discretizations have been applied to these global systems.

We have applied three types of interior penalty DG methods which are SIPG, NIPG and IIPG methods for the first example which is given in (1.1). For time discretization, we have used a fully implicit backward Euler method and a semi-implicit IMEX-BDF scheme. We have obtained numerical errors for u_1, u_2, u_3 and u_4. u_i's are the concentrations of four chemical species. These figures show that error decreases when the degree of DG approximation which is the degree of polynomials used in DG approximation increases. The slopes of error lines in the numerical errors figures give insight about convergence rates. For degree 1 and degree 2, convergence rates are about two. Degree 3 do not show improvement after a certain degree of freedom. Degree of freedom is the product of the number of elements and the local dimension($DoF = Nel * Nloc$). Numerical results of both time discretization methods are the same. We did not need to take very small time steps to obtain the same result. $\Delta t = 0.005$ was taken on $t = [0, 1]$ interval. Moreover, we have also obtained numerical solution plots with their error plots for both species. Numerical solutions approach to exact solutions which can be understood from error figures.

To analyze fully implicit and semi-implicit time discretization methods for ADR equations, then we have chosen river ecosystems with a unidirectional flow as another application area. We have solved two competing species advective LV model as an example to these systems. Lutscher [15] solved this problem by using numerical methods which are backward Euler method in time, finite difference method in space for the diffusion term and upwind for the advection term, however we solved this problem by using SIPG in space and by using fully implicit Euler method and semi-implicit IMEX-BDF method in time as in the previous chemical kinetics example.A semi-implicit method which is more efficient than fully implicit methods gave the same result without using smaller time steps. As in [15] after a short time, densities of both species decrease

upstream. The species 2 shows much more decrease than the species 1 at t=10. When time passes, species 1 catches its initial density in the upstream and species 2 is out of compete. We observe that a coexistence place between species occurs.

Finally, we have solved a problem from (2.3) which includes three competing species. Numerical results obtained by two time discretization methods are same. Decreases in the densities are seen for all species towards to the upstream after a short time. The reason, especially for species 2 and species 3, is the invasion to the downstream. The invasion speed of species 2 is faster than species 3 at the beginning. The density of species 2 decreases at the downstream when the density of species 3 increases at this part of the domain. Then, species 1 starts to move towards downstream slowly. There are time levels which coexistence between species occurs. After a while, each species catch their own balance densities.

In conclusion, We have obtained convergence rates of three DG methods and found that numerical solutions of the fully implicit BE method and semi-implicit IMEX-BDF method show the same dynamical behaviour for the competing species of advective LV models. A semi-implicit discretization is significantly larger according to explicit discretization, thus the computer time required to solve these equations is shorter. They have computational saving because the resulted scheme needs only the solution of linear part of our system in contrast to fully implicit methods. As a result, semi-implicit methods are advantageous for solving advective LV models.

REFERENCES

[1] G. Akrivis, Implicit–explicit multistep methods for nonlinear parabolic equations, Mathematics of Computation, 82(281), pp. 45 – 68, 2012.

[2] N. C. Apreutesei, An optimal control problem for a predator-prey reaction-diffusion system, Mathematical Modelling of Natural Phenomena, 5, pp. 180–195, 2010.

[3] D. N. Arnold, An interior penalty finite element method with discontinuous elements, SIAM J. Numer. Anal., 19(4), pp. 742–760, 1982.

[4] M. Ascher, S. Ruuth, and R. Spiteri, Implicit explicit runge kutta methods for time-dependent partial differential equations, Applied Numerical Mathematics, 25(2-3), pp. 151–167, 1997.

[5] B. Ayuso and L. D. Marini, Discontinuous Galerkin methods for advection-diffusion-reaction problems, SIAM J. Numer. Anal., 47(2), pp. 1391–1420, 2009.

[6] J. Hofbaeuer and K. Sigmund, *Evolutionary Games and Population Dynamics*, Bulletion Of The American Mathematical Society, 1998, ISBN 9780521625708.

[7] C. S. Holling, The components of predation as revealed by a study of small-mammal predation of the European pine sawfly, The Canadian Entomologist, 91, pp. 293–320, 5 1959, ISSN 1918-3240.

[8] C. S. Holling, Some characteristics of simple types of predation and parasitism, The Canadian Entomologist, 91, pp. 385–398, 1959.

[9] D. Jones, H. Smith, L. Dung, and M. Ballyk, Effects of random motility on microbial growth and competition in a flow reactor, SIAM Journal on Applied Mathematics, 59(2), pp. 573–596, 1998.

[10] K. Kishimoto, The diffusive Lotka-Volterra system with three species can have a stable non-constant equilibrium solution, Journal of Mathematical Biology, 16(1), 1982.

[11] I. Lagzi, D. Kàrmàn, T. Turànyi, A. Tomlin, and L. Haszpra, Simulation of the dispersion of nuclear contamination using an adaptive Eulerian grid model, Journal of Environmental Radioactivity, 75(1), pp. 59 – 82, 2004.

[12] I. Lagzi, R. Màszàros, L. Horvàth, A. Tomlin, T. Weidinger, T. Turànyi, F. Àcs, and L. Haszpra, Modelling ozone fluxes over Hungary, Atmospheric Environment, 38(36), pp. 6211 – 6222, 2004.

[13] B. Liu, An error analysis of a finite element method for a system of nonlinear advection diffusion reaction equations, Applied Numerical Mathematics, 59(8), pp. 1947–1959, 2009.

[14] A. J. Lotka, Analytical note on certain rhythmic relations in organic systems, Proceedings of the National Academy of Sciences of the United States of America, 6(7), pp. 410–415, 1920, ISSN 00278424.

[15] L. Lutscher, E. McCauley, and M. Lewis, Spatial patterns and coexistence mechanisms in systems with unidirectional flow, Theoretical Population Biology, 71(3), pp. 267 – 277, 2007.

[16] R. Mickens, A nonstandard finite-difference scheme for the lotka volterra system, Applied Numerical Mathematics, 45, pp. 309–314, 2003.

[17] V. W. Noonburg, A Neural Network Modeled by an Adaptive Lotka-Volterra System, SIAM J. Appl. Math., 49(6), pp. 1779–1792, 1989, ISSN 0036-1399.

[18] J. A. Pudykiewicz, Numerical solution of the reaction-advection-diffusion equation on the sphere, J. Comput. Phys., 213(1), pp. 358–390, 2006.

[19] W. H. Reed and T. R. Hill, Triangular mesh methods for the neutron transport equation, Technical Report LA-UR-73-479, Los Alamos Scientific Laboratory, 1973.

[20] H. Ritchie, Application of a Semi-Lagrangian Integration Scheme to the Moisture Equation in a Regional Forecast Model, American Meteorology Society, 113, pp. 424–435, 1985.

[21] B. Rivière, *Discontinuous Galerkin methods for solving elliptic and parabolic equations. Theory and implementation*, volume 35 of *Frontiers in Applied Mathematics*, Society for Industrial and Applied Mathematics (SIAM), Philadelphia, PA, 2008.

[22] B. Rivière, *Discontinuous Galerkin methods for solving elliptic and parabolic equations, Theory and implementation*, SIAM, 2008.

[23] J. Ruan and Z. Lu, A modified algorithm for the Adomian decomposition method with applications to Lotka–Volterra systems, Mathematical and Computer Modelling, 46(9–10), pp. 1214 – 1224, 2007.

[24] G. M. Scarpello and D. Ritelli, A new method for the explicit integration of Lotka-Volterra equations, Divulgaciones Matemticas, 11, pp. 1–17, 2003.

[25] E. Spee, J. Verwer, P. de Zeeuw, J. Blom, and W. Hundsdorfer, A numerical study for global atmospheric transport-chemistry problems, Mathematics and Computers in Simulation, 48(2), pp. 177–204, 1998.

[26] P. Sun, A pseudo-non-time-splitting method in air quality modeling, Journal of Computational Physics, 127(1), pp. 152–157, 1996.

[27] K.-i. Tainaka, Stationary pattern of vortices or strings in biological systems: Lattice version of the Lotka-Volterra model, Phys. Rev. Lett., 63, pp. 2688–2691, 1989.

[28] A. Tomlin, M. Berzins, J. Ware, J. Smith, and M. Pilling, On the use of adaptive gridding methods for modelling chemical transport from multi-scale sources, Atmospheric Environment, 31(18), pp. 2945 – 2959, 1997, ISSN 1352-2310.

[29] M. Uzunca, B. Karasözen, and M. Manguoğlu, Adaptive discontinuous galerkin methods for non-linear diffusion–convection–reaction equations, Computers & Chemical Engineering, 68, pp. 24 – 37, 2014.

[30] O. Vasilyeva and F. Lutscher, Competition of three species in an advective environment, Nonlinear Analysis: Real World Applications, 13(4), pp. 1730 – 1748, 2012.

[31] V. Volterra, *Variazioni e fluttuazioni del numero d'individui in specie animali conviventi*, Memoria CXXXI, Venice, Talass, Italiano, 1927.